Article

Study of Rolling Motion of Ships in Random Beam Seas with Nonlinear Restoring Moment and Damping Effects Using Neuroevolutionary Technique

Naveed Ahmad Khan [1] [ID], **Muhammad Sulaiman** [1,*] [ID], **Carlos Andrés Tavera Romero** [2] [ID], **Ghaylen Laouini** [3] and **Fahad Sameer Alshammari** [4,*] [ID]

1 Department of Mathematics, Abdul Wali Khan University, Mardan 23200, Pakistan; ahmednaveed854477@gmail.com
2 COMBA R&D Laboratory, Faculty of Engineering, Universidad Santiago de Cali, Cali 76001, Colombia; carlos.tavera00@usc.edu.co
3 College of Engineering and Technology, American University of the Middle East, Egaila 54200, Kuwait; ghaylen.laouini@aum.edu.kw
4 Department of Mathematics, College of Science and Humanities in Alkharj, Prince Sattam bin Abdulaziz University, Al-Kharj 11942, Saudi Arabia
* Correspondence: msulaiman@awkum.edu.pk (M.S.); f.alshammari@psau.edu.sa (F.S.A.)

Abstract: In this paper, a mathematical model for the rolling motion of ships in random beam seas has been investigated. The ships' steady-state rolling motion with a nonlinear restoring moment and damping effect is modeled by the nonlinear second-order differential equation. Furthermore, an artificial neural network (NN)-based, backpropagated Levenberg-Marquardt (LM) algorithm is utilized to interpret a numerical solution for the roll angle $(x(t))$, velocity $(x'(t))$, and acceleration $(x''(t))$ of the ship in random beam seas. A reference data set based on numerical examples of the mathematical model for a rolling ship for the LM-NN algorithm is generated by the numerical solver Runge–Kutta method of order 4 (RK-4). The LM-NN algorithm further uses the created data set for the validation, testing, and training of approximate solutions. The outcomes of the design paradigm are compared with those of the homotopy perturbation method (HPM), optimal homotopy analysis method (OHAM), and RK-4. Statistical analyses of the mean square error (MSE), regression, error histograms, proportional performance, and computational complexity further validate the worth of the LM-NN algorithm.

Keywords: steady-state roll motion; nonlinear damping; random beam seas; artificial neural networks; Levenberg-Marquardt algorithm; soft computing

1. Introduction

In general, ships experience different motions, including angular and displacement motions, categorized as yaw, pitch, roll, heave, drift, and surge. Figure 1 represents the schematic directions of all six motions. The stabilization of a ship depends on two methods, namely roll reduction and the modeling or evaluation method of roll performance. In the later part of the mid-18th century, Froude studied a ship's rolling motion for the first time. Later on, Norio Tanaka [1] introduced the empirical and semi-empirical roll damping coefficient for dynamic equations. A simple method was proposed by Himeno [2] for the prediction of the roll damping of ships at forwarding speed. In 2004, Ikeda [3] presented the modified model of roll damping with a steady drift motion.

In sea studies, roll damping is one of the important topics of discussion for most researchers. However, the complexity of problems and the potential flaws in traditional techniques make the solving of roll motion problems difficult. Scientists have adopted various strategies, including empirical formulas, advanced experimental processes, computational fluid dynamics (CDF), an analysis method for roll dumping, a finite differential

model, and a higher polynomial roll dumping model. Yeung [4] implemented a method based on CDF that had been used for local phenomena of vortex shedding around bilge keels. An experimental analysis on the local flow visualization of roll damping are given in [5–7].
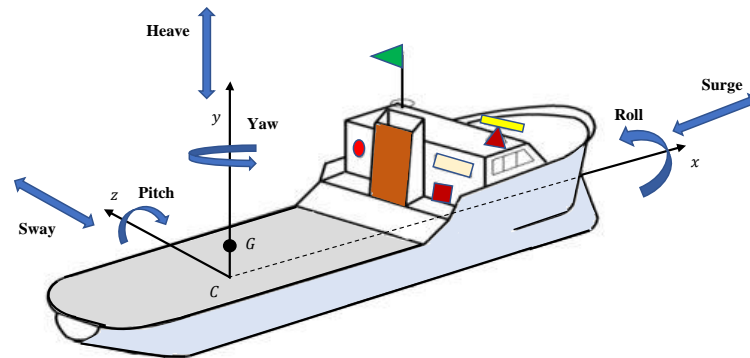

Figure 1. Schematic diagram of ship showing six directions of motion.

Researchers have recently focused on studying the mathematical modeling of the roll damping of ships. It has been noticed that external forces significantly affect ship stability, which causes complexity in mathematical models. The strong nonlinear terms arising in the mathematical model make it possible to study the behavior of forecasting stability changes in operations [8]. Oliveira and Fernandes [9] used the hyperbola or bilinear fitting method, and Agarwal [10], in 2015, used a fractional differential equation model to investigate the roll damping phenomena of ships. The ship's rolling motion in terms of a second-order nonlinear differential equation is of great significance to the research community. Finding a closed-form solution (exact solution) to such a model is difficult. Various numerical and perturbation techniques have been implemented to find the approximate solutions. Some well-established techniques for obtaining analytical expressions for roll angle, velocity, and acceleration are the finite element method (FEM) [11] ,differential transformation method (DTM) [12], homotopy analysis method (HAM) [13–15], variational iteration method (VIM) [16,17], homotopy perturbation method (HPM) [18], modified homotopy perturbation method [19], Green function-based method (GFM) [20], series method (SM) [21], and the ultraspherical wavelets-based method (UWM) [19]. Although these methods have advantages, especially over non-typical appendages in size and shape and newer hull designs, most of the methods are gradient-based techniques and depend on traditional deterministic approaches that have not been validated.

In recent times, stochastic optimization techniques based on artificial neural networks have been adopted to find numerical solutions to various complex and stiff problems. Recently, such soft computing techniques have been applied to study the wire coating phenomena [22], diabetic retinopathy classification using fundus images [23], imbibition phenomena [24], heat transfer in porous fins [25–27], wire coating dynamics [22], beam-column designs by varying axial load [28], absorption of carbon dioxide (CO_2) into solutions of phenyl glycidyl ether [29], mathematical models of CBSC over wireless channels [30], Michaelis–Menten kinetics in a micro-disk biosensor [31], a mathematical model for eye surgery [32], and electrohydrodynamic flow in a circular cylindrical conduit [33]. The techniques mentioned above have motivated the authors of this study to numerically solve the mathematical model of the ship's rolling motion by using a stochastic Levenberg-Marquardt (LM) algorithm based on neural networks that have never been applied to such a model. The potential outcomes of the presented work are summarized as follows:

- The formulation of a mathematical model for the rolling motion of ships in random beam seas will have been investigated;

- The novel, integrated design of a computing paradigm based on the two-layer structure of the Levenberg-Marquardt (LM) algorithm and neural networks (LM-NNs) is presented to examine the rolling motions;
- The model is briefly analyzed by considering certain examples depending on variations in angular frequency (ω_0^2), damping coefficient (μ), frequency (ω), amplitude (ϵ), and strength of nonlinearity coefficient (α);
- A merit function based on the mean square error is effectively developed for the computational analysis of LM-NNs by taking reference solutions of different examples generated by the RK-4 method;
- The training, testing, and validation process of LM-NNs are utilized to study the performance of approximate solutions by graphically illustrating regressions, absolute errors, and error histograms. The results of LM-NNs are compared with those of the HPM and RK-4 methods, which shows the dominance of the technique;
- An advantage of the proposed design is that it does not require any initial parameter settings. Its implementation is simple and smooth, with exhaustive applicability and stability.

2. Problem Formulation

In 1981, Cardo [34] formulated the mathematical equation for the rolling motion of a ship without any influence from oscillation, which is given as follows:

$$I\ddot{\xi} + M_r(\Theta, t) + D(\Theta, \dot{\Theta}) = E_W \cos \Omega t, \tag{1}$$

Equation (1) represents the general equation of the roll motion of ships in the absolute heeling angle, where ξ, $\dot{\xi}$, and $\ddot{\xi}$ denote the roll angle, velocity, and acceleration, respectively. The moment of inertia is denoted by I, D denotes the moment of forces, E_w is amplitude, M_r is the righting moment, and ω is the angular frequency. Here, the nonlinear damping term is taken into consideration as the angular dependence of the linear term, which is given by the following equation:

$$D(\xi, \dot{\xi}) = \left(D_{01} + D_{21}\xi^2\right)\dot{\xi} + D_{03}\dot{\xi}^3, \tag{2}$$

its normalized form of the righting moment can be expressed as:

$$M_r^*(\xi) = \omega_0^2 \xi + \alpha_3 \xi^3, \tag{3}$$

establishing dimensionless parameters by introducing the time T_n and angle ξ_n scales as follows:

$$\tau = \frac{t}{T_n}, \quad x = \frac{\xi}{\xi_n}, \quad \omega = \Omega T_n, \quad \omega_0^2 = \frac{\Delta k_1 T_n^2}{I}, \quad \delta_2 = \frac{D_{03}\phi_n^2}{IT_n},$$

$$\alpha_i = \Delta k_i T_n^2 \xi_n^{i-1}, \quad \delta_1 = \frac{D_{21}T_n \xi_n^2}{I}, \quad \mu = \frac{D_{01}T_n}{2I}, \quad \varepsilon = \frac{E_w T_n^2}{I\phi_n},$$

using the above parameters and rearranging the term gives the nonlinear equation of the cubic damping moment [34]:

$$\ddot{x} + \left(2\mu + \delta_1 x^2\right)\dot{x} + \delta_2 x^3 + \omega_0^2 x + \alpha_3 x^3 = \varepsilon \cos(\omega t). \tag{4}$$

where α, μ, ε, and ω denote the strength of nonlinearity, damping coefficient, amplitude, and angular frequency, respectively. δ_1 and δ_2 are viscous damping coefficients.

3. Proposed Methodology and Performance Indices

3.1. Structure of Artificial Neural Networks

Artificial neural networks (ANNs) are intelligent computational systems that mimic the biological nervous system. ANNs have been successfully applied by a number of

researchers to study the complex problems such as pattern identification, recognition, classification [35], electrical energy consumption forecasting [36], and induction motor drive in pumping [37].

The fundamental structure of ANNs comprises of interconnected neurons and nodes that receives the input, combines them in a specific way, and performs some nonlinear operation to generate the output. Figure 2 depicts the architecture of ANNs that consists of input, weight, threshold, summing junction, and output. For the basic model of ANNs, the input t_N is multiplied by the connection weights, and the bias or threshold is further applied to convert the inputs into the desired results. The net input is calculated as follows:

$$u_k = \sum_{k=1}^{N} w_k t_k - b_k. \tag{5}$$

In order to generate the output $x(t)$, an activation function such as Log-Sigmoid is used, which is given as:

$$x_k = f\left(\sum_{k=1}^{N} w_k t_k - B_k \right), \tag{6}$$
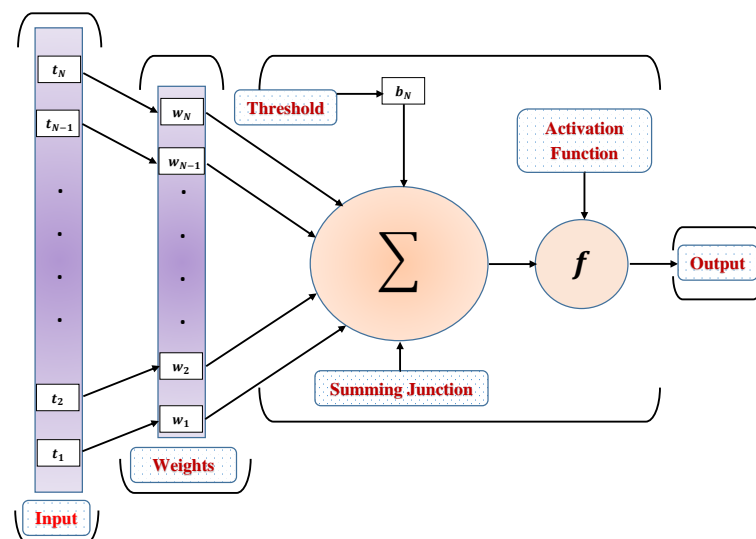
where N is the number of inputs.

Figure 2. Basic structure of a simple artificial neuron.

3.2. Learning Procedure

In this section, the learning procedure of the designed weights in the ANN structure is discussed. The implementation of the novel design of the Levenberg-Marquardt neural network approach is based on two steps. In the first step, a mathematical model for the rolling motion of the ship is evaluated by the Runge–Kutta method of order 4 using "NDSolve", the built in function of Mathematica to generate the reference solution of 301 data points, with a 0.1 step size from 0 to 30. In the second step, the Levenberg-Marquardt technique, which is an efficient technique in the field of soft computing, is implemented using the "nftool" routine on MATLAB for the proper training, validation, and testing of the problem. The work flow and parameter settings in terms of training, validation, and testing for the LM-NN algorithm is shown in Figure 3. The computational model with a double neural network for the design scheme has been plotted through Figure 4.
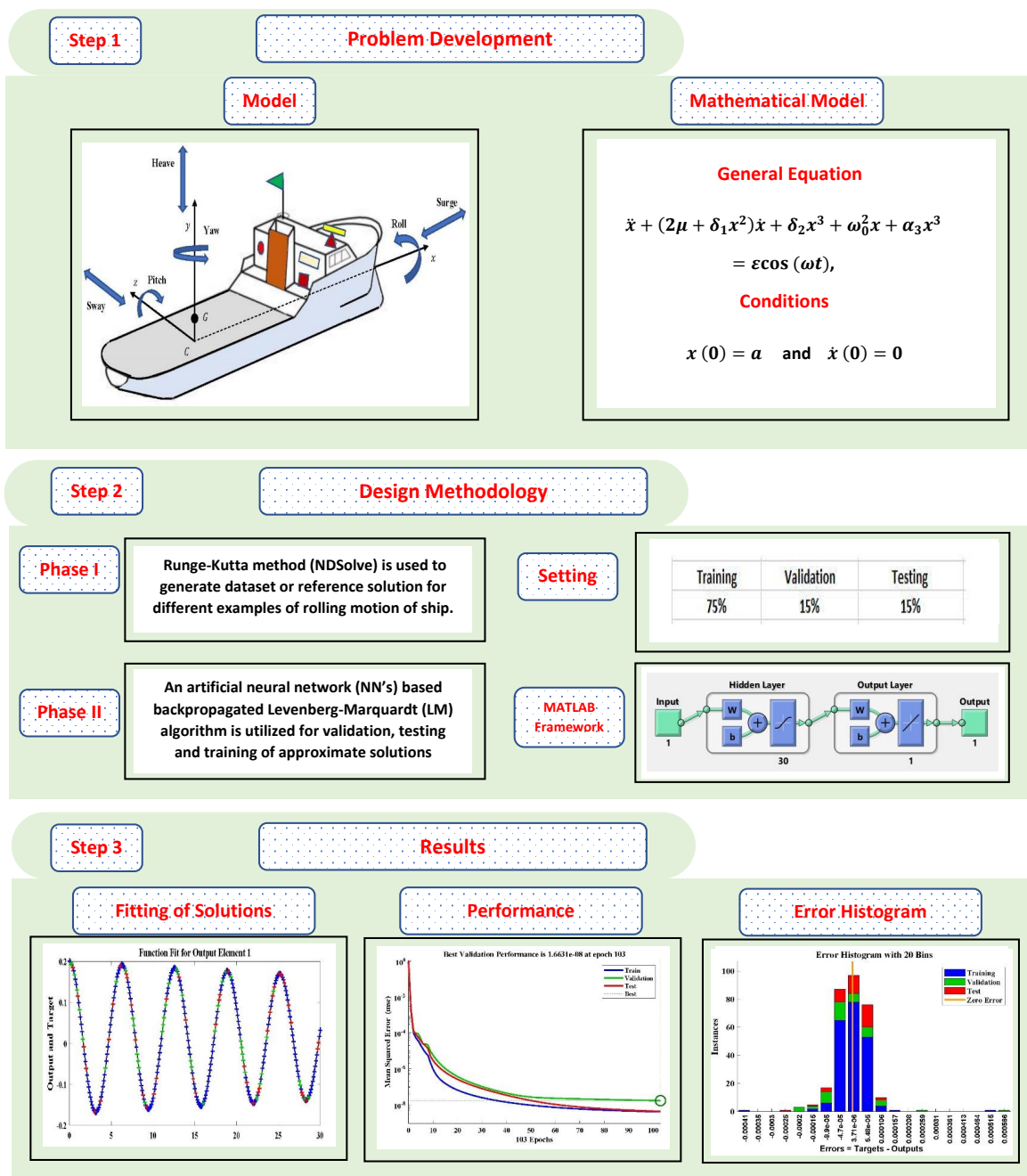
Figure 3. Architecture of the proposed methodology of the mathematical model for the rolling motion of ships in random beam seas.
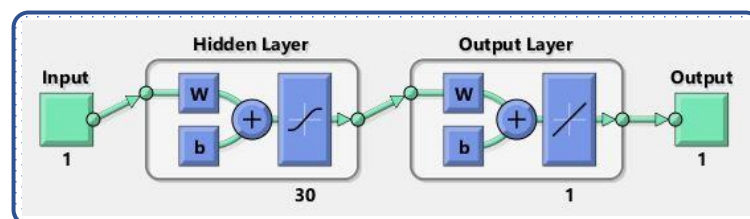

Figure 4. Structure of the supervised neural network [38].

The performance of the designed scheme is measured through the performance indicators in terms of the mean square error (MSE) of the fitness function of the model, regression

R^2, error histograms, and absolute errors (AE). The mathematical formulation of the MSE, R^2, and AE are given as follows:

$$\text{MSE} = \frac{1}{k} \sum_{j=1}^{k} \left(x_j(t) - \hat{x}_j(t) \right)^2, \tag{7}$$

$$R^2 = 1 - \frac{\sum_{j=1}^{k} \left(\hat{x}_j(t) - \bar{x}_j(t) \right)^2}{\sum_{j=1}^{k} \left(x_j(t) - \bar{x}_j(t) \right)^2}, \tag{8}$$

and

$$\text{AE} = \left| x_j(t) - \hat{x}_j(t) \right|, \quad j = 1, 2, \ldots, k, \tag{9}$$

where x_j, $\bar{x}_j$, and $\hat{x}_j$ denote the reference, approximate, and mean of the solution at the jth input, and k is the number of mesh points. The desired value for the MSE and AE for perfect fitting is equal to zero, while the value of R^2 is one.

4. Numerical Experimentation

In this section, we considered certain examples of the rolling motion of ships in random beam seas by varying certain parameters. Figure 5 shows the flow chart of the problems discussed in this paper.
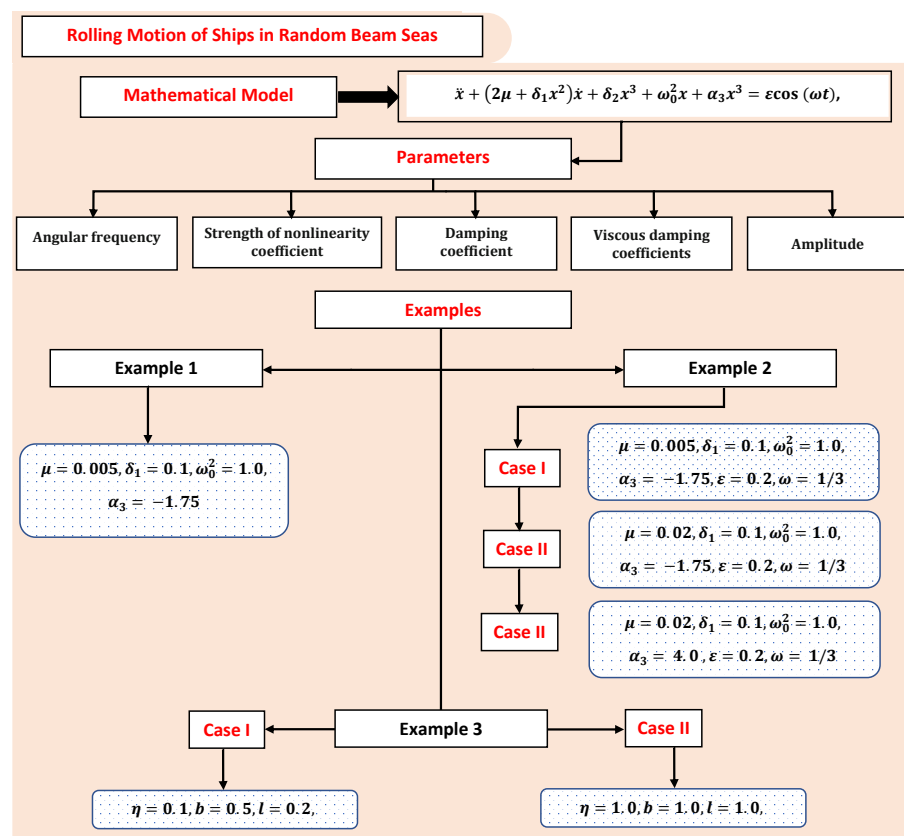

Figure 5. An overview of different examples and cases studied in this paper.

Example 1. *In this example, a nonlinear differential equation for the rolling motion of ships is considered* [19,34]:

$$\ddot{x} + \left(2\mu + \delta_1 x^2 \right) \dot{x} + \omega_0^2 x + \alpha_3 x^3 = 0, \tag{10}$$

subjected to

$$x(0) = a \quad and \quad \dot{x}(0) = 0. \tag{11}$$

Experimental values of the parameters involved in Equation (10) are $\delta_1 = 0.1$, $\mu = 0.005$, $\alpha_3 = -1.75$, $a = 0.2$, and $\omega_0^2 = 1$.

Example 2. *In this example, a nonlinear IVP of the cubic damping moment of the rolling motion is considered [34], which is given as follows:*

$$\ddot{x} + \left(2\mu + \delta_1 x^2\right)\dot{x} + \omega_0^2 x + \alpha_3 x^3 = \varepsilon \cos(\omega t), \tag{12}$$

with the initial conditions

$$x(0) = 0.2 \quad and \quad \dot{x}(0) = 0. \tag{13}$$

Furthermore, to briefly study the model, the following three cases are considered, depending on variations in the dimensionless damping coefficient and the strength of the nonlinearity coefficient. Case I : $\delta_1 = 0.1$, $\mu = 0.005$, $\alpha_3 = -1.75$, $\omega_0^2 = 1$, $\varepsilon = 0.2$, and $\omega = 0.333333$. Case II : $\delta_1 = 0.1$, $\mu = 0.02$, $\alpha_3 = -1.75$, $\omega_0^2 = 1$, $\varepsilon = 0.2$, and $\omega = 0.333333$. Case III : $\delta_1 = 0.1$, $\mu = 0.02$, $\alpha_3 = 4.0$, $\omega_0^2 = 1$, $\varepsilon = 0.2$, and $\omega = 0.333333$.

Example 3. *In this example, we considered the cubic damping moment of the nonlinear roll motion [14,39], which is given by the following equation:*

$$\ddot{x}\left(1 + 4b^2 x^2\right) + \eta x + 4b^2 x^2 x = 0, \quad \eta > 0, \tag{14}$$

with

$$x(0) = l \quad and \quad \dot{x}(0) = 0. \tag{15}$$

Two cases of Equation (14) are considered. Case I: $b = 0.5$, $\eta = 0.1$, and $l = 0.2$. Case II: $b = 1.0$, $\eta = 1.0$, and $l = 1.0$.

Chaos Phenomena of Ship Nonlinear Rolling Motion

When a ship is sailing, the motion of the ship is extremely complex. However, the large restoring and nonlinear torques cannot be ignored. AH Nayfeh [40], in 1990, took nonlinear damping and restoring torques into consideration and investigated the complexity and stability of the dynamics in the rolling motion of ships under the influence of different slopes and wave surfaces. The mathematical model for the nonlinear motion of ships subjected to the regular waves can be written as follows [41,42]:

$$(I + I^*)\ddot{\xi} + D(\dot{\xi}) + M(\xi) = B_1 - M(\dot{\alpha}, \ddot{\alpha}), \tag{16}$$

where $M(\dot{\alpha}, \ddot{\alpha})$ represents the wave disturbance torque, and α denotes the slope or gradient of the wave surfaces and is defined as:

$$\alpha = \alpha_m \cos(\omega t), \tag{17}$$

here, α_m is the maximum slope. The chaotic phenomena are extremely sensitive, particulary to the external disturbances, therefore the $M(\dot{\alpha}, \ddot{\alpha})$ can be given as follows:

$$M(\dot{\alpha}, \ddot{\alpha}) = -f_1 \alpha_m \omega \sin \omega t - f_2 \alpha_m \omega^2 \cos \omega t, \tag{18}$$

where $f_1 \alpha_m \omega \sin \omega t$ and $f_2 \alpha_m \omega^2 \cos \omega t$ are the restoring and damping disturbance torques. Equation (17) is reduced to the following equation:

$$(I + I^*)\ddot{\xi} + D(\dot{\xi}) + M(\xi) = B_1 + f_1 \alpha_m \omega \sin \omega t + f_2 \alpha_m \omega^2 \cos \omega t, \tag{19}$$

$D(\dot{\xi})$ and $M(\xi)$ can be given as:

$$D(\dot{\xi}) = 2\mu_1 \dot{\xi} + \mu_3 \dot{\xi}^3, \tag{20}$$

$$M(\xi) = \omega_0^2 \xi + \alpha_3 \xi^3 + \alpha_5 \xi^5 + \dots, \tag{21}$$

here, $2\mu_1$ and μ_3 are linear and cubic damping coefficients of torque. Moreover, α_3, α_5 are constants and ω_0^2 is the linear restoring coefficient of torque. B_1 is constant, and its value can be calculated as follows:

$$B_1 = \omega_0 \xi_s + \alpha_3 \xi_s + \alpha_5 \xi_s, \tag{22}$$

where ξ_s represents the heeling angle. Using Equations (20)–(22) in Equation (19) will result in the following:

$$(I + I^*)\ddot{\xi} + 2\mu_1 \dot{\xi} + \mu_3 \dot{\xi}^3 + \omega_0^2 \xi + \alpha_3 \xi^3 + \alpha_5 \xi^5 = f_1 \alpha_m \omega \sin \omega t + f_2 \alpha_m \omega^2 \cos \omega t. \tag{23}$$

The mathematical model is simplified by introducing dimensionless parameters such as:

$$m_1 = \frac{2\mu_1}{I + I^*}, m_2 = \frac{\mu_3}{I + I^*}, n_1 = \frac{\omega_0^2}{I + I^*}, n_2 = \frac{\alpha_3}{I + I^*}, n_3 = \frac{\alpha_5}{I + I^*}, A_1 = \frac{f_1}{I + I^*}, \text{ and } A_2 = \frac{f_2}{I + I^*}. \tag{24}$$

Equation (23) can be given as follows:

$$\ddot{\xi} + m_1 \dot{\xi} + m_2 \dot{\xi}^3 + n_1 \xi + n_2 \xi^3 + n_3 \xi^5 = A_1 \alpha_m \omega \sin \omega t + A_2 \alpha_m \omega^2 \cos \omega t. \tag{25}$$

Values of the parameters involved in Equation (25) are given in Table 1. One of the primary characteristics of a chaotic system is that there is great sensitivity to the initial values. The traces formed by the small difference between the two initial values will disperse in the usual way as time goes on [43]. Equation (25) is similar to duffing equations, which are strongly nonlinear and are commonly used for detecting the weak signals in the chaotic systems. Furthermore, to study the chaos phenomena in ships, Equation (25) is reduced to the system of differential equations by letting $x = \xi, y = \dot{\xi}$, and $z = \omega t$:

$$\begin{cases} \dot{x} - y = 0, \\ \dot{y} = -3.240x + 4.5250x^3 - 0.8780x^5 - 0.3500y - 0.0222y^3 + 0.5040\alpha_m \omega \sin z - 4.6656\alpha_m \omega^2 \cos z, \\ \dot{z} - \omega = 0, \end{cases} \tag{26}$$

with the initial conditions

$$x(0) = y(0) = 0, \text{ and } z(0) = 1. \tag{27}$$

Table 1. Values of parameters involved in the mathematical model for the rolling of ships given in Equation (25).

Parameters	n_1	n_2	n_3	m_1	m_2	A_1	A_2
Values	3.24	−4.525	0.878	0.35	0.0222	0.504	−4.6656

5. Results and Discussion

In this section, the implementation of the proposed LM-NN algorithm to solve the mathematical model for the rolling motion of ships in random beam seas is discussed. Numerical and graphical results are illustrated for all three mathematical examples with different cases. An approximate solution for each example obtained by the LM-NNs is compared with those of the homotopy perturbation method (HPM) [19], the Runge–Kutta method (RK-4), and the optimal homotopy analysis method (OHAM) [39], as shown in Figure 6. Tables 2 and 3 represent the statistics of the obtained values for the rolling angle, velocity, and acceleration. The behaviour of variations in different parameters on $\dot{x}(t)$ and $\ddot{x}(t)$ are shown in Figure 7. Figure 8 illustrates rolling decay curves that show the impact of time on the rolling angle. Furthermore, to study the chaotic behaviour of the rolling motion of ships, Equation (26) is solved by the LM-NNs to study the influence of variation on maximum slope α_m. Figure 9a shows the frequency spectrum diagram of the motion. It can be observed that increasing the value of α_m causes an increase in the rolling angle of

the ship. The system's dispersion phenomena become obvious, and the rolling angle of the ship's motion increases correspondingly. Figure 9a analyzes the chaotic behaviour of the rolling motion of ships.

The design scheme is exploited to determine the fitting of approximate solutions, with the reference date set generated from the numerical solver using the RK-4 method. Curve fitting of the obtained solutions by LM-NNs for each example, with reference data of 301 points from 0 to 30, is shown in Figure 10. The performance of the objective function in terms of MSE to obtain best fitting is depicted in Figure 11. The best validated performance of MSE for different examples are 1.6631×10^{-8}, 4.4759×10^{-9}, 2.9493×10^{-9}, 1.0449×10^{-9}, 5.7951×10^{-10}, and 1.1029×10^{-8}, respectively. Figure 12 represents the absolute errors between the reference solution and the approximated solution by the LM-NN algorithm. It can be seen that the AE for different examples lies at around 10^{-4} to 10^{-6}, 10^{-5} to 10^{-6}, 10^{-4} to 10^{-6}, 10^{-5} to 10^{-6}, 10^{-5} to 10^{-6}, and 10^{-4} to 10^{-5}, respectively. These plots show the convergence, precision, and accuracy of LM-NNs for obtaining solutions to the mathematical model for the cubic damping of the rolling motion of ships.

Regression values for each example are illustrated in Figures 13 and 14. The correlation investigation was applied to study the regression analysis. The figures and Table 4 demonstrate that the value of "R" lies close to one, which reflects the perfect modeling of the solutions by the LM-NN algorithm. Figure 15 shows that values of the gradient and step size of mu for each example lies at around 9.9599×10^{-8}, 9.5875×10^{-8}, 9.9596×10^{-8}, 9.9867×10^{-8}, 9.1618×10^{-8}, and 6.3457×10^{-7}, with 10^{-10}, 10^{-11}, 10^{-11}, 10^{-11}, 10^{-12}, and 10^{-9}, respectively. Finally, all calculations and evaluations for this research were performed on an HP laptop EliteBook 840 G2 with intel(R) Core (TM) i5-5300 CPU @ 2.30 GHz, 8.00 GB RAM, 64 bit operating in Microsoft Windows 10 Education edition, running an R2018a version of MATLAB. The time taken by the CPU to solve such complex problems by the LM-NN algorithm are shown in Table 4.
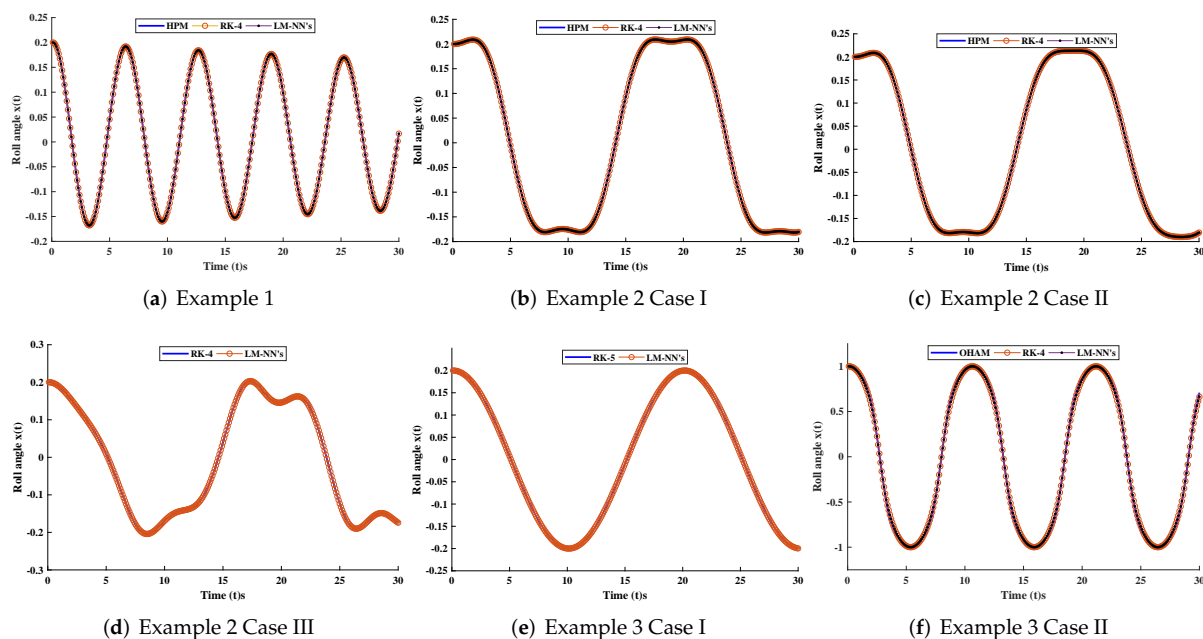

(a) Example 1

(b) Example 2 Case I

(c) Example 2 Case II

(d) Example 2 Case III

(e) Example 3 Case I

(f) Example 3 Case II

Figure 6. Comparison of approximate solutions with the numerical solver (RK-4), HPM, and OHAM for different examples of the rolling motion of ships.
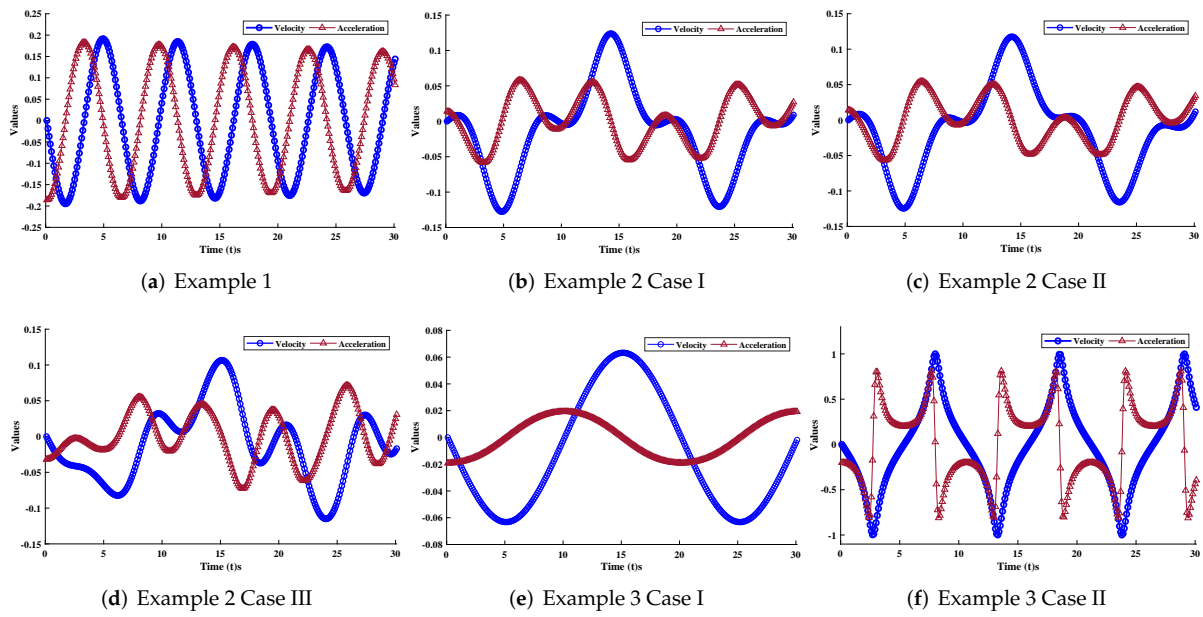
Figure 7. Plots of velocity $\dot{x}(t)$ and acceleration $\ddot{x}(t)$ for different cases of the cubic damping motion of ships in random beam seas.
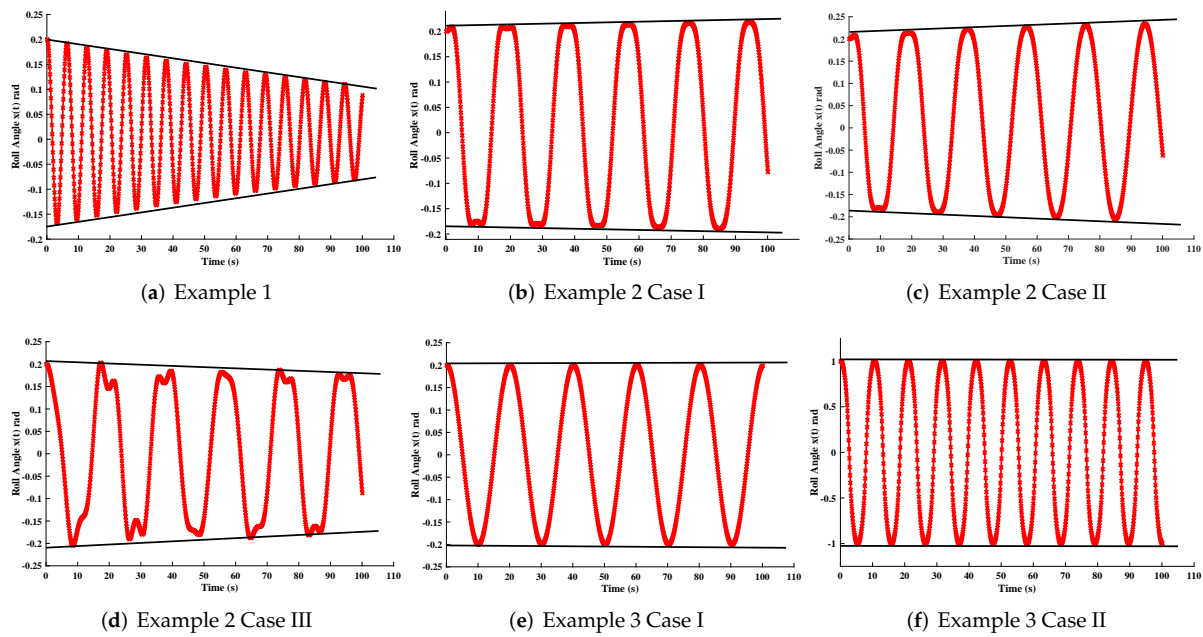

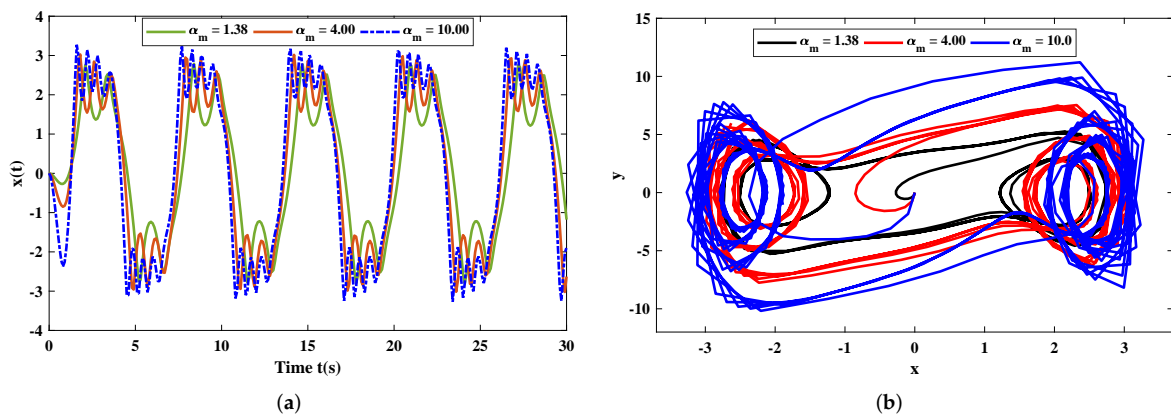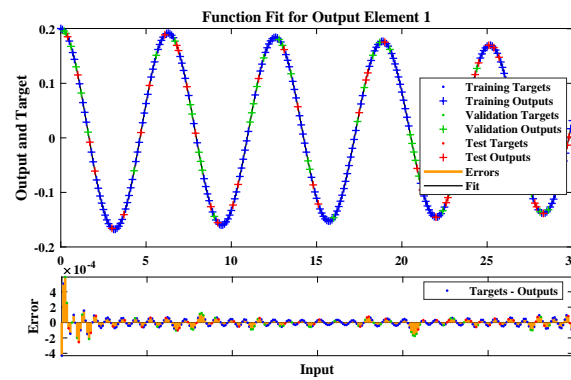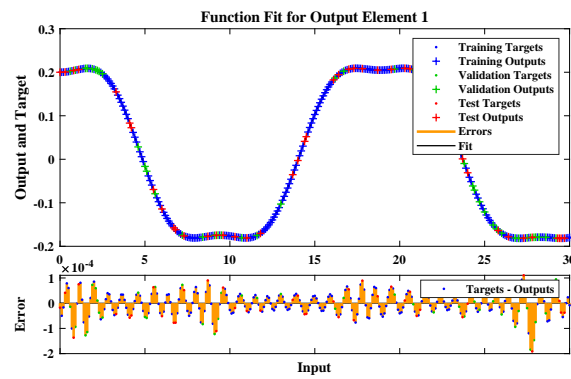**Figure 8.** Roll angle decay curves for each example.

Figure 9. (**a**) Demonstrates the influence of variations in α_m on the rolling motion of ships. (**b**) Phase-space diagram of $y(t)$ against $x(t)$ for different values of the maximum slope.
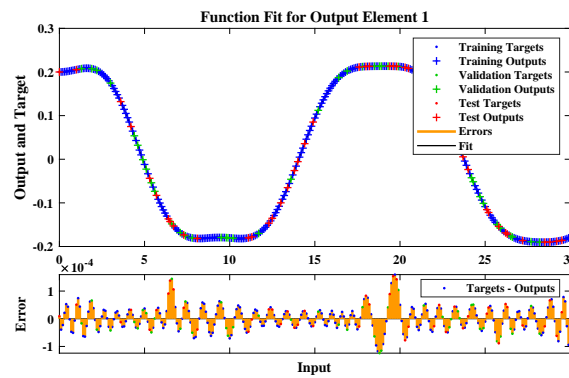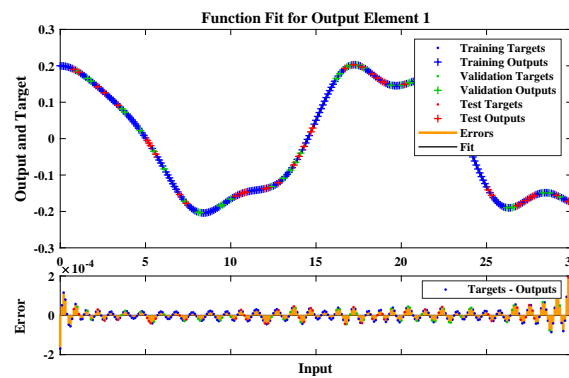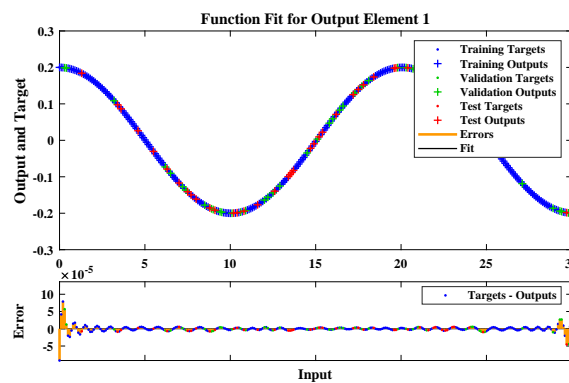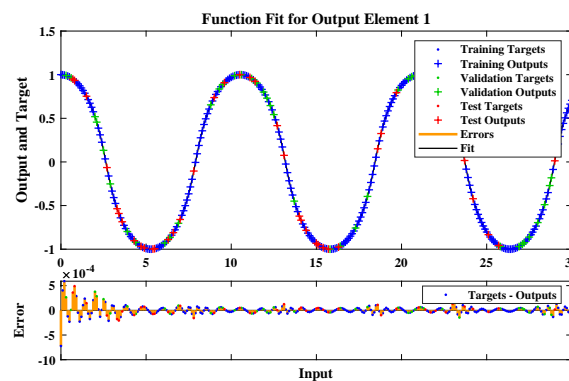

(**a**) Example 1

(**b**) Example 2 Case I

Figure 10. *Cont.*

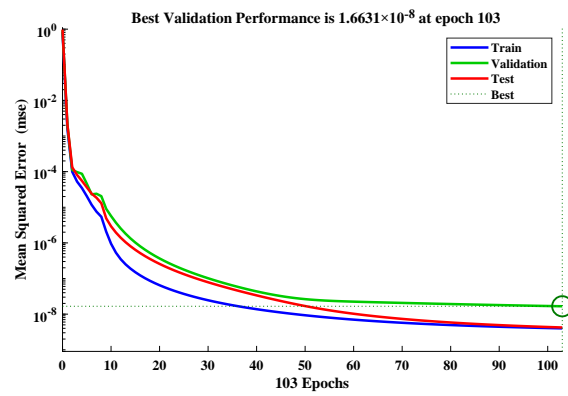(**c**) Example 2, Case II

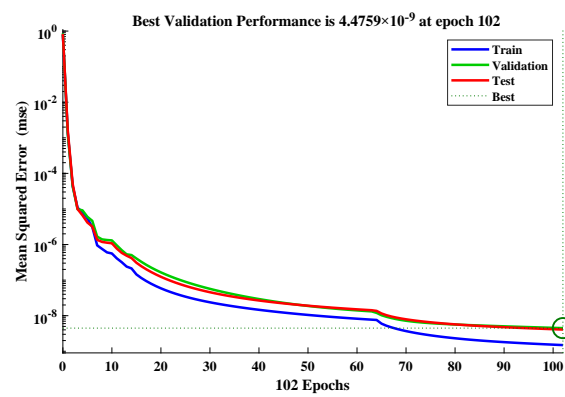(**d**) Example 2, Case III

(**e**) Example 3, Case I

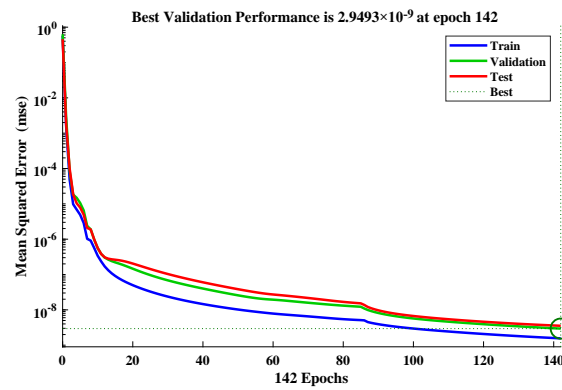(**f**) Example 3, Case II

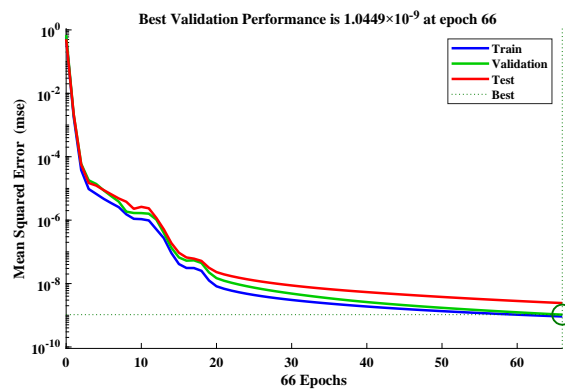**Figure 10.** Analysis of the fitness plot by the LM-NN algorithm for different examples.

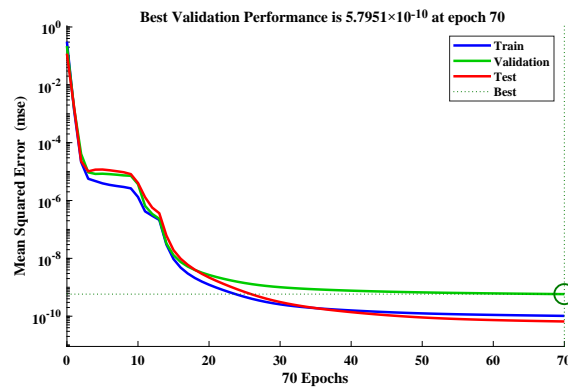(**a**) Example 1
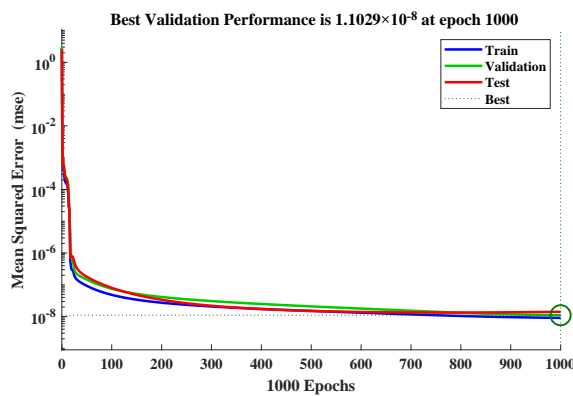

(**b**) Example 2, Case I

(**c**) Example 2, Case II

(**d**) Example 2, Case III.

Figure 11. *Cont.*

Best Validation Performance is 5.7951×10⁻¹⁰ at epoch 70

(**e**) Example 3, Case I

**Best Validation Performance is 1.1029×10⁻⁸ at epoch 1000**
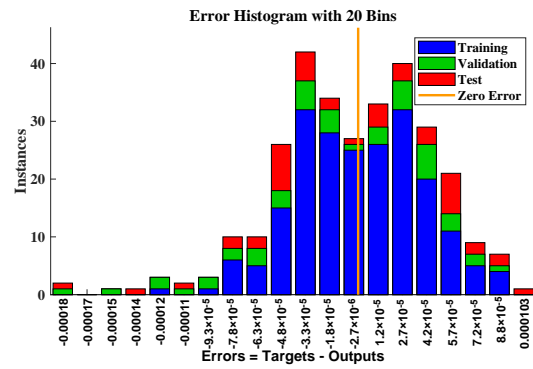
(**f**) Example 3, Case II

Figure 11. Studies based on the performance of MSE by the design scheme, for multiple examples.

Table 2. Approximate solutions obtained by the LM-NN algorithm for different examples of the rolling motion of ships in random beam seas.
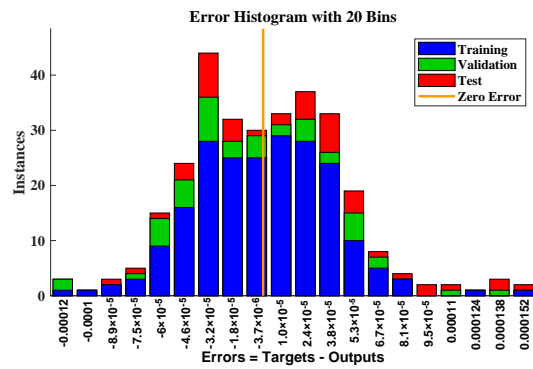
	Example 1			Example 2			Example 3		
				Case I	Case II	Case III	Case I	Case II	
t	MHPM	Anaytical	LM-NN's					OHAM	LM-NN's
0	0.2	0.2	0.2	0.2	0.2	0.2	0.2	1	1
3	−0.166120	−0.191740	−0.191730	0.176480	0.176568	0.109021	0.118817	−0.338480	−0.334040
6	0.184868	0.174917	0.174914	−0.142790	−0.136060	−0.075050	−0.061160	−0.941280	−0.945690
9	−0.144550	−0.150800	−0.150820	−0.205370	−0.209320	−0.196250	−0.189810	0.775350	0.737937
12	0.157559	0.120891	0.120810	−0.191980	−0.190840	−0.137690	−0.163790	0.798647	0.767593
15	−0.112290	−0.086840	−0.086850	0.097787	0.091824	0.050338	−0.003150	−0.931210	−0.932550
18	0.121196	0.050406	0.050406	0.210881	0.210487	0.188166	0.160140	−0.398350	−0.395290
21	−0.072730	−0.013330	−0.013320	0.202523	0.207454	0.160958	0.191669	0.999319	0.999335
24	0.079358	−0.022720	−0.022720	−0.050090	−0.050840	−0.027350	0.067115	−0.27570	−0.267520
27	−0.029550	0.056298	0.056296	−0.210560	−0.203030	−0.179030	−0.113730	−0.950850	−0.957320
30	0.035768	−0.086160	−0.086160	−0.211550	−0.221450	−0.175970	−0.199900	0.749124	0.705858
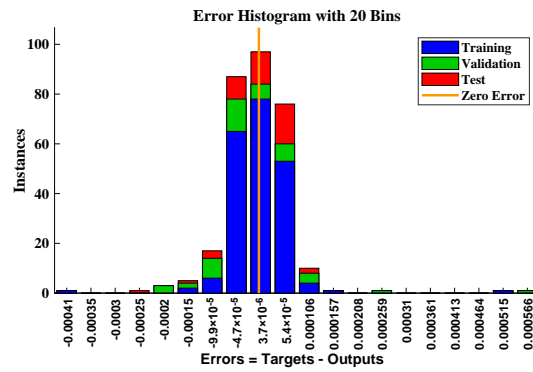
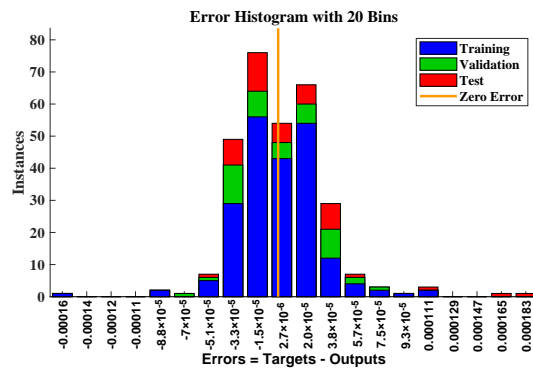(**a**) Example 1
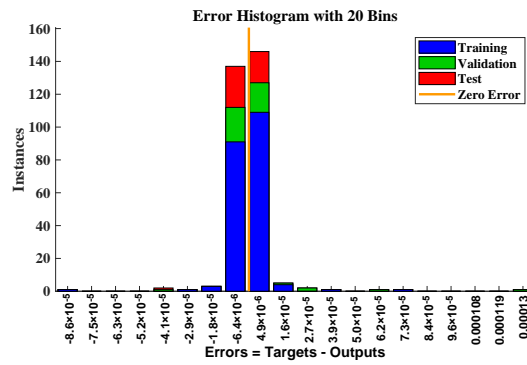

(**b**) Example 2, Case I
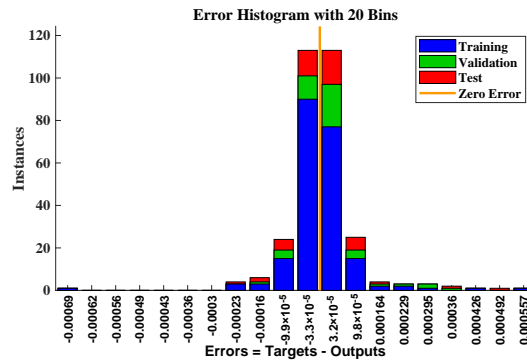

(**c**) Example 2, Case II

(**d**) Example 2, Case III

Figure 12. *Cont.*

(**e**) Example 3, Case I

(**f**) Example 3, Case II

Figure 12. Error histograms, representing absolute errors between the reference solution and the approximated solution for different examples of the rolling motion of ships in random beam seas.
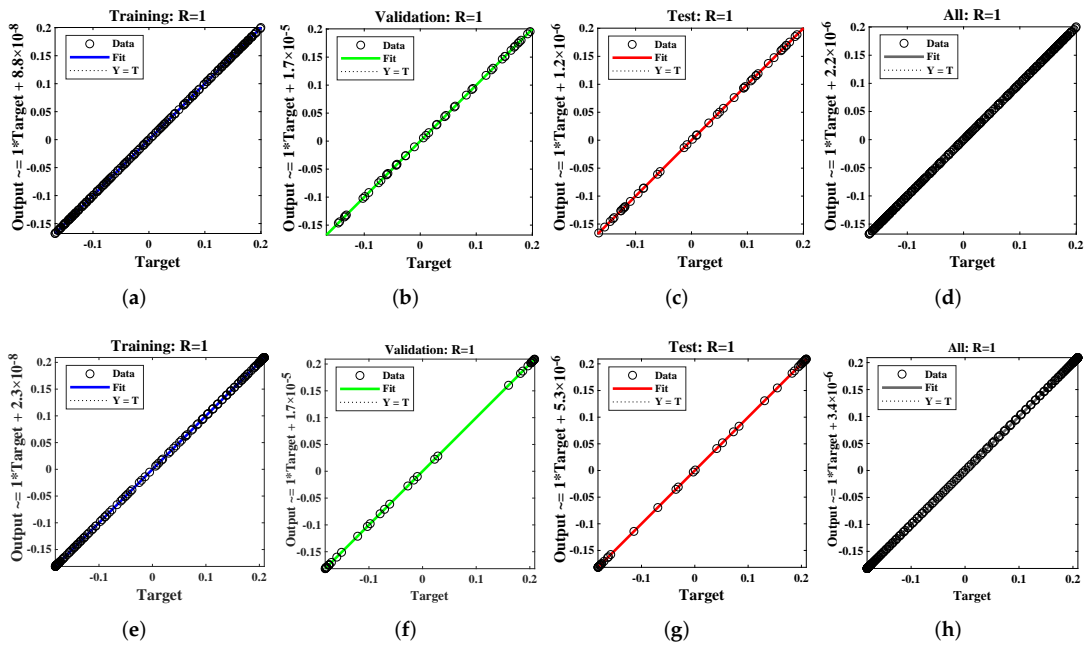

Figure 13. *Cont.*
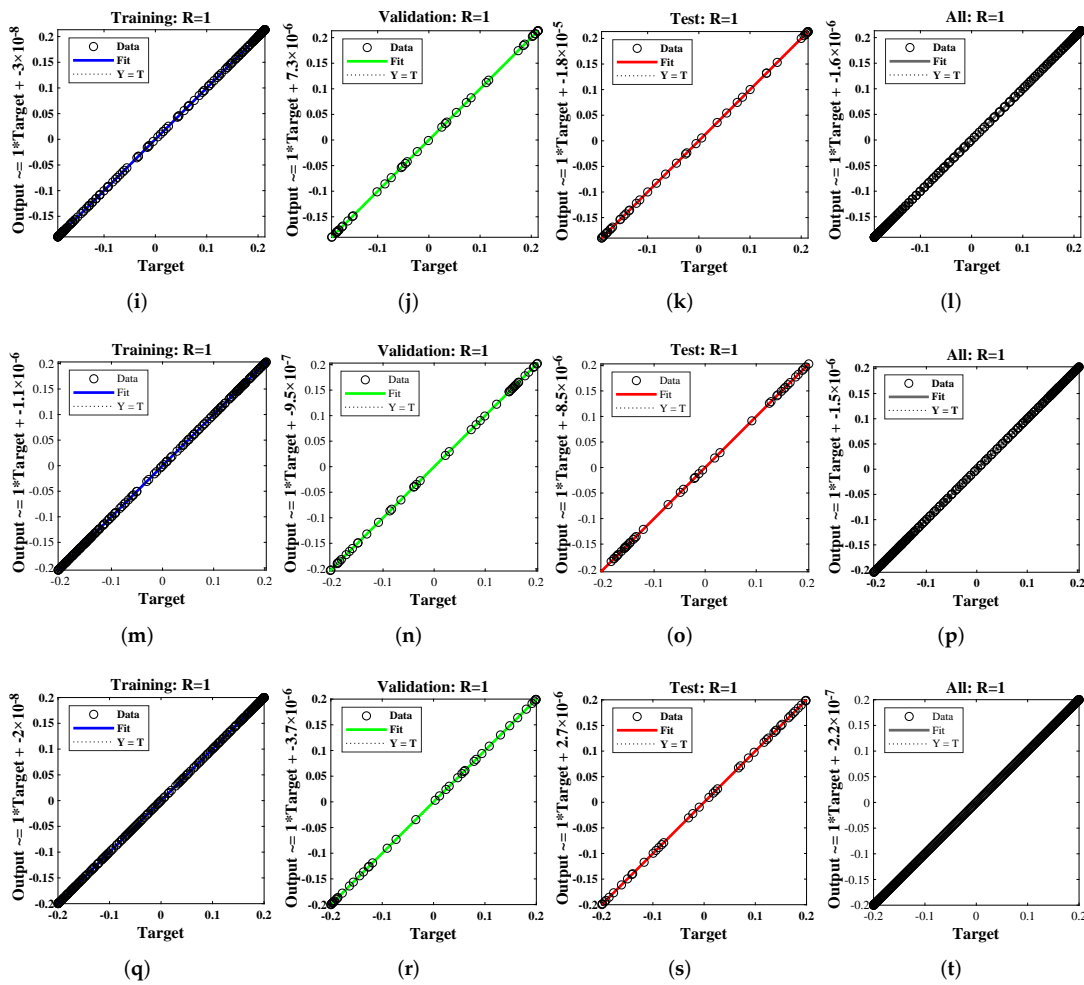
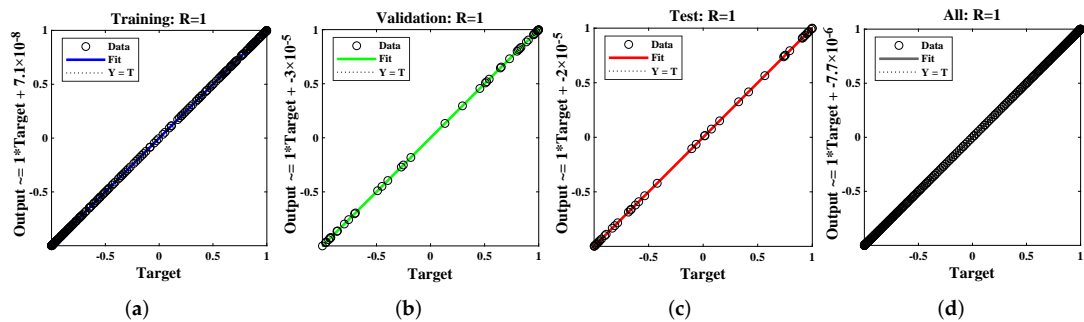**Figure 13.** Regression analysis of Examples 1 and 2.

Figure 14. Regression analysis of Example 3.

Table 3. Results of velocity $\dot{x}(t)$ and acceleration $\ddot{x}(t)$ for different examples of the rolling motion of ships.

| | Example 1 | | Example 2 | | | | | | Example 3 | | | |
| | | | Case I | | Case II | | Case III | | Case I | | Case II | |
t	$\dot{x}(t)$	$\ddot{x}(t)$	$\dot{x}(t)$	$\ddot{x}(t)$	$\dot{x}(t)$	$\ddot{x}(t)$	$\dot{x}(t)$	$\ddot{x}(t)$	$\dot{x}(t)$	$\ddot{x}(t)$	$\dot{x}(t)$	$\ddot{x}(t)$
3	−0.04120	0.17996	−0.05802	−0.05804	−0.05705	−0.05641	−0.04287	−0.00438	−0.05052	−0.01202	−0.78374	0.79843
9	−0.11206	0.14617	0.00643	−0.00788	0.00253	−0.00484	0.02417	0.02742	−0.01958	0.01839	0.37855	−0.36528
18	0.17082	−0.05193	−0.00528	−0.00236	0.00324	−0.00228	−0.03384	−0.02131	0.03741	−0.01583	0.72057	0.74845
27	−0.16067	−0.05433	−0.00085	0.01201	−0.00809	0.00652	0.02764	0.01857	−0.05169	0.01152	0.13380	0.80846

Table 4. Statistical analysis of the performance measures, including MSE, Gradient, mu, number of iterations, and time taken by the system to calculate the results.

| Example	Case	Hidden Neurons	Mean Square Error			Gradient	Mu	Epochs	Regression	Time (s)
			Training	Testing	Validation					
1		30	3.98×10^{-9}	1.66×10^{-8}	4.22×10^{-9}	9.96×10^{-8}	1.00×10^{-10}	103	1	<1 s
2	I	30	1.49×10^{-9}	4.48×10^{-9}	4.07×10^{-9}	9.59×10^{-8}	1.00×10^{-11}	102	1	<1 s
2	II	30	1.56×10^{-9}	2.95×10^{-9}	3.54×10^{-9}	9.69×10^{-8}	1.00×10^{-11}	142	1	<1 s
2	III	30	9.15×10^{-10}	1.04×10^{-9}	2.42×10^{-9}	9.99×10^{-8}	1.00×10^{-11}	66	1	<1 s
3	I	30	1.02×10^{-10}	5.80×10^{-10}	6.57×10^{-11}	9.16×10^{-8}	1.00×10^{-12}	70	1	<1 s
3	II	30	9.08×10^{-9}	1.10×10^{-8}	1.42×10^{-8}	6.35×10^{-7}	1.00×10^{-9}	1000	1	1 s
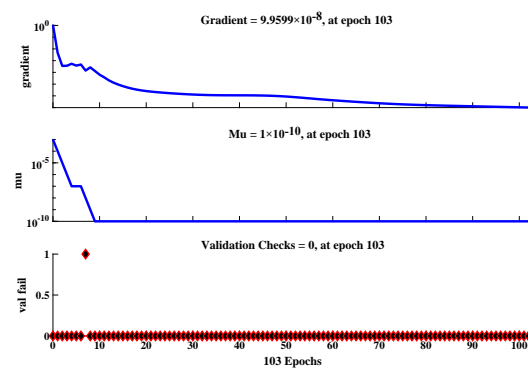
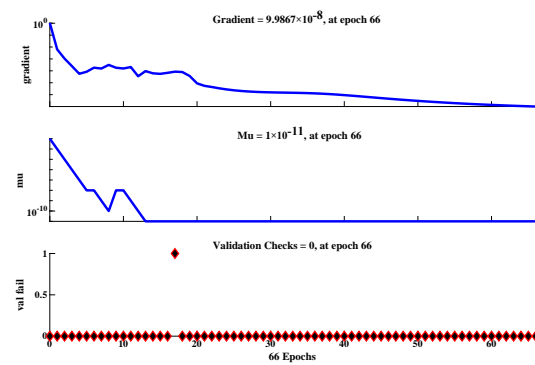(**a**) Example 1
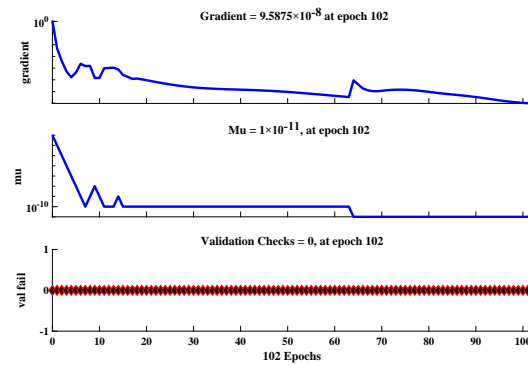
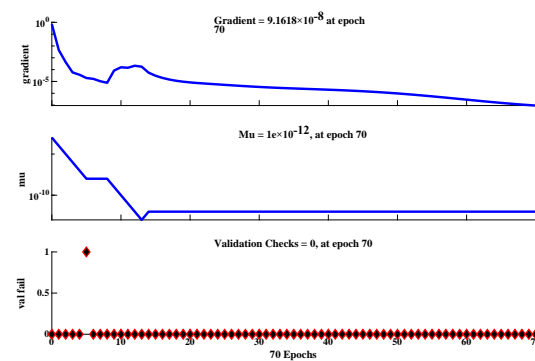(**b**) Example 2, Case I
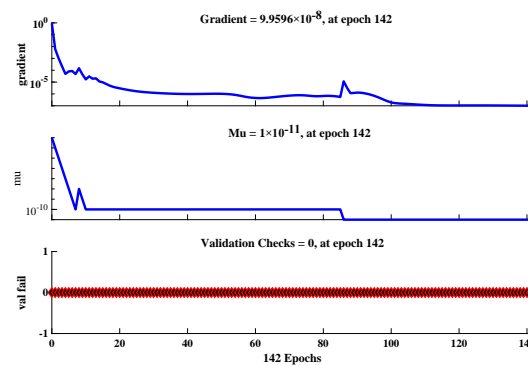
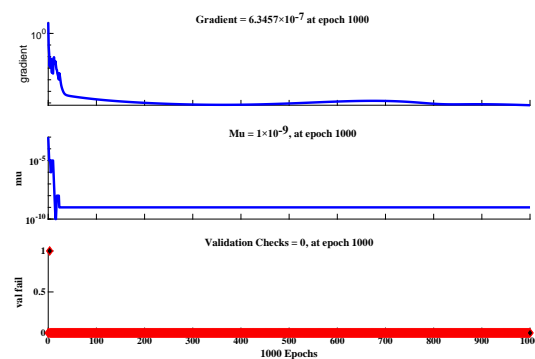

(**c**) Example 2, Case II

Figure 15. *Cont.*

(**d**) Example 2, Case III

(**e**) Example 3, Case I

(**f**) Example 3, Case II

Figure 15. Training state of the design scheme for all examples of the rolling motion.

6. Conclusions

This paper analyzes a mathematical model of the rolling motion of ships with nonlinear damping in random beam seas. To study the roll motion of ships under the effect of various forces and parameters, including angular frequency, strength of the nonlinearity coefficient, damping coefficient, viscous damping coefficients, and amplitude, we developed an intelligent soft computing technique based on artificial neural networks. A novel computing paradigm with a two-layer structure, the Levenberg-Marquardt (LM) algorithm and neural networks were utilized to calculate the approximate solution to the mathematical model by using a data set generated by numerical solvers such as the Runge–Kutta method or Adam's method. Reference solutions of 70%, 15%, and 15% were utilized by the LM-NNs for the training, validation, and testing of the numerical examples. The results obtained by the proposed LM-NN algorithm were compared with those of the homotopy perturbation method (HPM), the Runge–Kutta method (RK-4), and the optimal homotopy analysis method (OHAM). Furthermore, to study the chaotic behavior of the rolling motion of ships, the mathematical model was solved by the LM-NNs to study the influence of

variation on maximum slope α_m. The results demonstrate that increasing the value of α_m causes an increase in the rolling angle of the ship. The system's dispersion phenomena become apparent, and the rolling angle of the ship's motion increases correspondingly. The technique's performance is disclosed in terms of mean square error (MSE), regression R^2, error histograms, and performance evaluation. Extensive graphical and statistical results show the technique's accuracy, precision, and robustness.

In the future, the designed scheme can be used to implement the solving of partial and fractional differential equations representing real-world problems.

Author Contributions: Conceptualization, N.A.K.; Formal analysis, N.A.K.; Funding acquisition, F.S.A.,G.L. and C.A.T.R.; Investigation, N.A.K. and M.S.; Methodology, N.A.K. and M.S.; Project administration, M.S.; Resources, F.S.A., G.L. and C.A.T.R., M.S.; Software, M.S.; Supervision, M.S.; Visualization, N.A.K.; Writing—original draft, N.A.K.; Writing—review and editing, N.A.K., F.S.A., G.L., C.A.T.R. and M.S. All authors have read and agreed to the published version of the manuscript.

Institutional Review Board Statement: Not applicable.

Informed Consent Statement: Not applicable.

Data Availability Statement: The data that support the findings of this study are available from the corresponding author upon reasonable request.

Conflicts of Interest: The authors declare that they have no competing interests.

References

1. Tanaka, N. A Study on the Bilge Keels. *J. Zosen Kiokai* **1961**, *1961*, 205–212. [CrossRef]
2. Himeno, Y. Prediction of Ship Roll Damping—A State of the Art 1981. Available online: https://deepblue.lib.umich.edu/handle/2027.42/91699 (accessed on 20 June 2021).
3. Ikeda, Y.; Ali, B.; Yoshida, H. A roll damping prediction method for a FPSO with steady drift motion. In Proceedings of the Fourteenth International Offshore and Polar Engineering Conference, Toulon, France, 23–28 May 2004.
4. Yeung, R.; Cermelli, C.; Liao, S. Vorticity fields due to rolling bodies in a free surface—Experiment and theory. In Proceedings of the 21st Symposium on Naval Hydrodynamics, Trondheim, Norway, 24–28 June 1996.
5. Bassler, C.C.; Carneal, J.B.; Atsavapranee, P. Experimental investigation of hydrodynamic coefficients of a wave-piercing tumblehome hull form. In Proceedings of the International Conference on Offshore Mechanics and Arctic Engineering, San Diego, CA, USA, 10–15 June 2007; Volume 42703, pp. 537–548.
6. De Oliveira, A.C.; Fernandes, A.C. An empirical nonlinear model to estimate FPSO with extended bilge keel roll linear equivalent damping in extreme seas. In Proceedings of the International Conference on Offshore Mechanics and Arctic Engineering, Rio de Janeiro, Brazil, 1–6 July 2012; Volume 44915, pp. 413–428.
7. Aloisio, G.; Felice, F. PIV analysis around the bilge keel of a ship model in free roll decay. *Convegno Naz. AI VE LA* **2006**, *14*, 1–11.
8. Lihua, L.; Peng, Z.; Songtao, Z.; Ming, J.; Jia, Y. Simulation analysis of fin stabilizer on ship roll control during turning motion. *Ocean. Eng.* **2018**, *164*, 733–748. [CrossRef]
9. De Oliveira, A.C.; Carlos Fernandes, A. The nonlinear roll damping of a FPSO hull. *J. Offshore Mech. Arct. Eng.* **2014**, *136*, 011106. [CrossRef]
10. Agarwal, D. A Study on the Feasibility of Using Fractional Differential Equations for Roll Damping Models. Ph.D. Thesis, Virginia Tech, Blacksburg, VA, USA, 2015.
11. Comini, G.; Del Guidice, S.; Lewis, R.; Zienkiewicz, O. Finite element solution of non-linear heat conduction problems with special reference to phase change. *Int. J. Numer. Methods Eng.* **1974**, *8*, 613–624. [CrossRef]
12. Chen, C.; Liu, Y. Solution of two-point boundary-value problems using the differential transformation method. *J. Optim. Theory Appl.* **1998**, *99*, 23–35. [CrossRef]
13. Liao, S. Homotopy analysis method: A new analytical technique for nonlinear problems. *Commun. Nonlinear Sci. Numer. Simul.* **1997**, *2*, 95–100. [CrossRef]
14. Liao, S.J.; Chwang, A. Application of homotopy analysis method in nonlinear oscillations. *J. Appl. Mech.* **1998**, *65*, 914–922. [CrossRef]
15. Liao, S. On the homotopy analysis method for nonlinear problems. *Appl. Math. Comput.* **2004**, *147*, 499–513. [CrossRef]

16. Lu, J. Variational iteration method for solving a nonlinear system of second-order boundary value problems. *Comput. Math. Appl.* **2007**, *54*, 1133–1138. [CrossRef]
17. Abukhaled, M. Variational iteration method for nonlinear singular two-point boundary value problems arising in human physiology. *J. Math.* **2013**. [CrossRef]
18. He, J. Comput Methods Appl. *Mech. Engrg.* **1999**, *178*, 257.
19. Selvi, M.S.M.; Rajendran, L.; Abukhaled, M. Estimation of Rolling Motion of Ship in Random Beam Seas by Efficient Analytical and Numerical Approaches. *J. Mar. Sci. Appl.* **2021**, *20*, 1–12. [CrossRef]
20. Abukhaled, M.; Khuri, S. A semi-analytical solution of amperometric enzymatic reactions based on Green's functions and fixed point iterative schemes. *J. Electroanal. Chem.* **2017**, *792*, 66–71. [CrossRef]
21. Salomi, R.J.; Sylvia, S.V.; Rajendran, L.; Abukhaled, M. Electric potential and surface oxygen ion density for planar, spherical and cylindrical metal oxide grains. *Sens. Actuators B Chem.* **2020**, *321*, 128576. [CrossRef]
22. Khan, N.A.; Sulaiman, M.; Kumam, P.; Aljohani, A.J. A new soft computing approach for studying the wire coating dynamics with Oldroyd 8-constant fluid. *Phys. Fluids* **2021**, *33*, 036117. [CrossRef]
23. Ali, A.; Qadri, S.; Khan Mashwani, W.; Kumam, W.; Kumam, P.; Naeem, S.; Goktas, A.; Jamal, F.; Chesneau, C.; Anam, S.; et al. Machine learning based automated segmentation and hybrid feature analysis for diabetic retinopathy classification using fundus image. *Entropy* **2020**, *22*, 567. [CrossRef]
24. Khan, N.A.; Sulaiman, M.; Aljohani, A.J.; Kumam, P.; Alrabaiah, H. Analysis of Multi-Phase Flow Through Porous Media for Imbibition Phenomena by Using the LeNN-WOA-NM Algorithm. *IEEE Access* **2020**, *8*, 196425–196458. [CrossRef]
25. Khan, N.A.; Khalaf, O.I.; Romero, C.A.T.; Sulaiman, M.; Bakar, M.A. Application of Euler Neural Networks with Soft Computing Paradigm to Solve Nonlinear Problems Arising in Heat Transfer. *Entropy* **2021**, *23*, 1053. [CrossRef]
26. Ahmad, A.; Sulaiman, M.; Alhindi, A.; Aljohani, A.J. Analysis of temperature profiles in longitudinal fin designs by a novel neuroevolutionary approach. *IEEE Access* **2020**, *8*, 113285–113308. [CrossRef]
27. Khan, N.A.; Sulaiman, M.; Kumam, P.; Bakar, M.A. Thermal analysis of conductive-convective-radiative heat exchangers with temperature dependent thermal conductivity. *IEEE Access* **2021**, *9*, 138876–138902. [CrossRef]
28. Huang, W.; Jiang, T.; Zhang, X.; Khan, N.A.; Sulaiman, M. Analysis of Beam-Column Designs by Varying Axial Load with Internal Forces and Bending Rigidity Using a New Soft Computing Technique. *Complexity* **2021**, *2021*. [CrossRef]
29. Khan, N.A.; Sulaiman, M.; Tavera Romero, C.A.; Alarfaj, F.K. Theoretical Analysis on Absorption of Carbon Dioxide (CO_2) into Solutions of Phenyl Glycidyl Ether (PGE) Using Nonlinear Autoregressive Exogenous Neural Networks. *Molecules* **2021**, *26*, 6041. [CrossRef]
30. Khan, N.A.; Sulaiman, M.; Aljohani, A.J.; Bakar, M.A.; Miftahuddin. Mathematical models of CBSC over wireless channels and their analysis by using the LeNN-WOA-NM algorithm. *Eng. Appl. Artif. Intell.* **2022**, *107*, 104537. [CrossRef]
31. Khan, N.A.; Alshammari, F.S.; Romero, C.A.T.; Sulaiman, M.; Laouini, G. Mathematical Analysis of Reaction–Diffusion Equations Modeling the Michaelis–Menten Kinetics in a Micro-Disk Biosensor. *Molecules* **2021**, *26*, 7310. [CrossRef]
32. Waseem, W.; Sulaiman, M.; Alhindi, A.; Alhakami, H. A soft computing approach based on fractional order DPSO algorithm designed to solve the corneal model for eye surgery. *IEEE Access* **2020**, *8*, 61576–61592. [CrossRef]
33. Khan, N.A.; Sulaiman, M.; Tavera Romero, C.A.; Alarfaj, F.K. Numerical Analysis of Electrohydrodynamic Flow in a Circular Cylindrical Conduit by Using Neuro Evolutionary Technique. *Energies* **2021**, *14*, 7774. [CrossRef]
34. Cardo, A.; Francescutto, A.; Nabergoj, R. Ultraharmonics and subharmonics in the rolling motion of a ship: Steady-state solution. *Int. Shipbuild. Prog.* **1981**, *28*, 234–251. [CrossRef]
35. Hasni, A.; Sehli, A.; Draoui, B.; Bassou, A.; Amieur, B. Estimating global solar radiation using artificial neural network and climate data in the south-western region of Algeria. *Energy Procedia* **2012**, *18*, 531–537. [CrossRef]
36. Ahmad, A.S.; Hassan, M.Y.; Abdullah, M.P.; Rahman, H.A.; Hussin, F.; Abdullah, H.; Saidur, R. A review on applications of ANN and SVM for building electrical energy consumption forecasting. *Renew. Sustain. Energy Rev.* **2014**, *33*, 102–109. [CrossRef]
37. Ebrahim, O.S.; Badr, M.A.; Elgendy, A.S.; Jain, P.K. ANN-based optimal energy control of induction motor drive in pumping applications. *IEEE Trans. Energy Convers.* **2010**, *25*, 652–660. [CrossRef]
38. Available online: https://www.mathworks.com/help/deeplearning/gs/fit-data-with-a-neural-network.html (accessed on 3 August 2021).
39. Marinca, V.; Herişanu, N. Determination of periodic solutions for the motion of a particle on a rotating parabola by means of the optimal homotopy asymptotic method. *J. Sound Vib.* **2010**, *329*, 1450–1459. [CrossRef]
40. Nayfeh, A.; Sanchez, N. Stability and complicated rolling responses of ships in regular beam seas. *Int. Shipbuild. Prog.* **1990**, *37*, 177–198.
41. Pu, J.Y.; Liu, H.; Wu, X.J.; Chen, X.H. Experimental study in nonlinear rolling motion of a flooded ship. *J. Ship Mech.* **2011**, *5*, 2537–2553.
42. Yu, Y.; Shenoi, R.A.; Zhu, H.; Xia, L. Using wavelet transforms to analyze nonlinear ship rolling and heave-roll coupling. *Ocean. Eng.* **2006**, *33*, 912–926. [CrossRef]
43. Llibre, J.; Rodrigues, A. A non-autonomous kind of Duffing equation. *Appl. Math. Comput.* **2015**, *251*, 669–674. [CrossRef]